LOAN DOCUMENT

PHOTOGRAPH THIS SHEET

DTIC ACCESSION NUMBER

LEVEL

INVENTORY

NADC-76200-30

~~IR-6154-007~~

DOCUMENT IDENTIFICATION

DISTRIBUTION STATEMENT

HANDLE WITH CARE

ACCESSION FOR

NTIS GRA&I

DTIC TRAC

UNANNOUNCED

JUSTIFICATION

BY

DISTRIBUTION/

AVAILABILITY CODES

DISTRIBUTION	AVAILABILITY AND/OR SPECIAL	
A-1		

DISTRIBUTION STAMP

DATE ACCESSIONED

DATE RETURNED

19981223 044

DATE RECEIVED IN DTIC

REGISTERED OR CERTIFIED NUMBER

PHOTOGRAPH THIS SHEET AND RETURN TO DTIC-FDAC

DTIC FORM 70A JUN 90

DOCUMENT PROCESSING SHEET

PREVIOUS EDITIONS MAY BE USED UNTIL STOCK IS EXHAUSTED.

LOAN DOCUMENT

IRT 6154-001

PRELIMINARY FEASIBILITY EVALUATION OF NEUTRON RADIOGRAPHY FOR DETECTING CRACKS IN TITANIUM COMPRESSOR BLADES FROM TF-30 AIRCRAFT ENGINES

BY

HOWARD HARPER AND JOSEPH JOHN
IRT CORP.

PREPARED FOR

OKLAHOMA AIR LOGISTIC CENTER
U. S. AIR FORCE
OKLAHOMA CITY, OKLAHOMA

UNDER

CONTRACT N62269-76-C-0165

WITH

ANALYTICAL REWORK/SERVICE LIFE PROJECT OFFICE
NAVAL AIR DEVELOPMENT CENTER
WARMINSTER, PENNSYLVANIA 18974

OCTOBER 7, 1976

CONTENTS

LIST OF ILLUSTRATIONS

Figure

1. INTRODUCTION

The F-111 and the F-14 aircraft are both powered by the same basic engine; *viz.* the TF-30 jet engine manufactured by Pratt and Whitney Aircraft Company. Several catastrophic failures have been reported recently which were attributed to cracks in the titanium first-stage compressor blades. This has made it necessary to carefully inspect these blades at regular intervals. At the present time, this requires the expenditure of a significant number of maintenance manhours to carry out an effective inspection of each blade.

The purpose of this study was to carry out a preliminary evaluation of the feasibility of detecting cracks in titanium compressor blades utilizing neutron radiography. These defects, namely cracks, were artificially introduced to such an extent that many were detectable by careful visual inspection under a microscope, thereby providing a means of quantitizing the results from the neutron radiographs. For this reason, only those areas containing defects were radiographed for this study.

Several techniques were used to enhance the detection of these defects for neutron radiography. One of these techniques involved the use of introducing a penetrant in the cracks, the thermal-neutron absorption cross section of which was quite different from the titanium base material. In this technique, it is hoped that a sufficient amount of penetrant would be in the defects and subsequently be detected on the neutron radiograph because of its different thermal-neutron cross section. The other technique examined involved the use of electroplating a material on the cracked areas of the blade with the expectation that the cracks would perturb the electric fields sufficiently to produce a significant amount of plated material. The material plated was one whose thermal-neutron cross section was quite different from the titanium base material. In the plating technique, it is hoped that the electroplated material would be detected in the deposited areas only, which should enhance the contrast around the crack itself.

2. BACKGROUND DISCUSSION

Neutron radiography is a nondestructive inspection technique that is similar in principle to x ray, in that penetrating radiation (neutrons) is used to obtain a visual image of the internal form of an object. The transmitted neutron beam is detected and permanently recorded on an imaging system. This imaging system consists of a material (gadolinium) that converts the impinging neutrons to electrons, which subsequently interact with normal x-ray film to obtain an image.

Although x ray and neutron radiography are similar in principle, the difference in their respective absorption coefficients for various materials makes neutron radiography particularly useful. This is particularly so when trying to discern between two different materials, as is the case when using the penetrant or electroplating technique for the detection of cracks.

Thermal neutrons are most widely used because of their higher probability of interaction with most materials, thereby making them easier to detect and offering the best contrast between elements of interest and the surrounding medium.

A neutron beam is attenuated in any material according to

$$I = I_0 e^{-\Sigma t} \quad ,$$

where I is the radiation intensity transmitted through a material having a thickness t, and a linear absorption or attenuation coefficient Σ, and I_0 is the initial radiation intensity. Naturally, it would be desirable to relatively change Σ for the path along which the desired defect is located. In the case of using a penetrant, a gadolinium salt solution is introduced in the crack. Gadolinium has one of the highest attenuation coefficients for thermal neutrons. For the case of the electroplating

technique, a thin deposited layer of gadolinium serves to give the negative response of the penetrant technique, in that the beam is now more easily transmitted through the crack due to the absence of the gadolinium.

The following examples are considered to show the benefits of utilizing a material with such a high thermal-neutron attenuation coefficient. Consider the examples of a titanium sample approximately 0.125 inch thick (Case 1) and another of the same thickness with an additional 0.0005-inch layer of gadolinium (Case 2). For these examples, we give the following parameters.

Total attenuation coefficient for gadolinium thickness, $\Sigma = 70\ cm^{-1}$.

Total attenuation coefficient for titanium, $\Sigma = 0.12\ cm^{-1}$.

For Case 1, the transmission ratio is

$$I/Io = e^{-\Sigma t}_{sample} = e^{-0.12 \times 0.125 \times 2.54} = 0.963 \quad .$$

For Case 2, the transmission ratio is

$$I/Io = \left(e^{-\Sigma t}_{sample}\right) \cdot \left(e^{-\Sigma t}_{gadolinium\ layer}\right)$$

$$I/Io = 0.963 \cdot \left(e^{-70 \times 5 \times 10^{-4} \times 2.54}\right) = 0.88 \quad .$$

The relative transmission ratios between both of these cases, when considering a radiograph of background density near 2.0, are easily discernible.

This demonstrates the fact that density differences due to either a penetrant or an electrodeposited layer can be detected.

3. EQUIPMENT, METHODS, AND MATERIALS

3.1 CFNR-10 NEUTRON RADIOGRAPHY SYSTEM

The CFNR-10 system consists of the neutroscope, imaging system, and beam stop, which are illustrated in Figure 1. The performance characteristics of the system are described in Table 1, which include the thermal-neutron flux density.

3.1.1 Neutroscope (Neutron Camera)

The neutroscope is shown schematically in Figure 2, illustrating the main camera components, which are the biological shield, source tube, moderator, collimators, and shutter. The biological shield, which makes up the bulk of the camera, is required to permit personnel to work in close proximity of the system.

Figure 3 illustrates the moderator, precollimator, collimator, and shutter. The moderator is composed of high-density polyethylene which slows down fission neutrons from ^{252}Cf to thermal energies. Since the entire polyethylene becomes the source of thermal neutrons, an aperture is introduced into the middle of the moderator near the source. The neutrons exit from the moderator through this aperture to a precollimator consisting of a thermal-neutron absorber. This collimator captures those neutrons that would otherwise scatter into the imaging system. The aperture then looks at the imaging plane through a divergent collimator, further defining the neutron beam by capturing scattered neutrons. An annular ring of lead reduces the number of gamma rays from the source and moderator reaching the imaging plane.

The source tube contains the four single sources of ^{252}Cf used to obtain the initial neutron spectrum. Figure 4 illustrates the locations of the four sources in the operating and storage positions. The storage position is used if, for some reason, the camera shutter must be opened with personnel in that area.

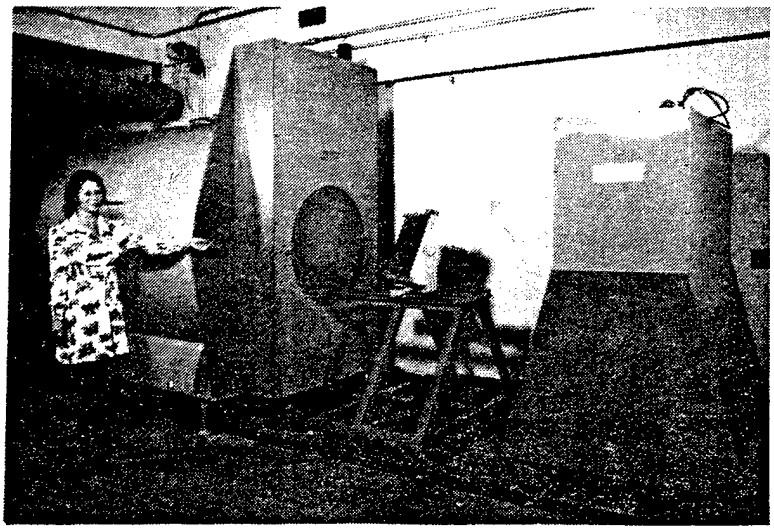

Figure 1. CFNR-10 system (left to right) neutroscope (CFNR-10), imaging system (IS-10), and beam stop (BS-10)

Table 1

PERFORMANCE CHARACTERISTICS OF CFNR-10 SYSTEM

Source	31.0 mg ^{252}Cf
L/D Ratios	Variable 14 to 80
Thermal-neutron flux (2200 m/sec)	3.4×10^4 n/cm^2-sec at L/D = 20
Cadmium Ratio	45.7:1
Dose (total γ and n) at camera surface with sources in stored position	Side: 59.6 mrem Back: 39.1 mrem Top: 44.1 mrem Front: 50 mrem

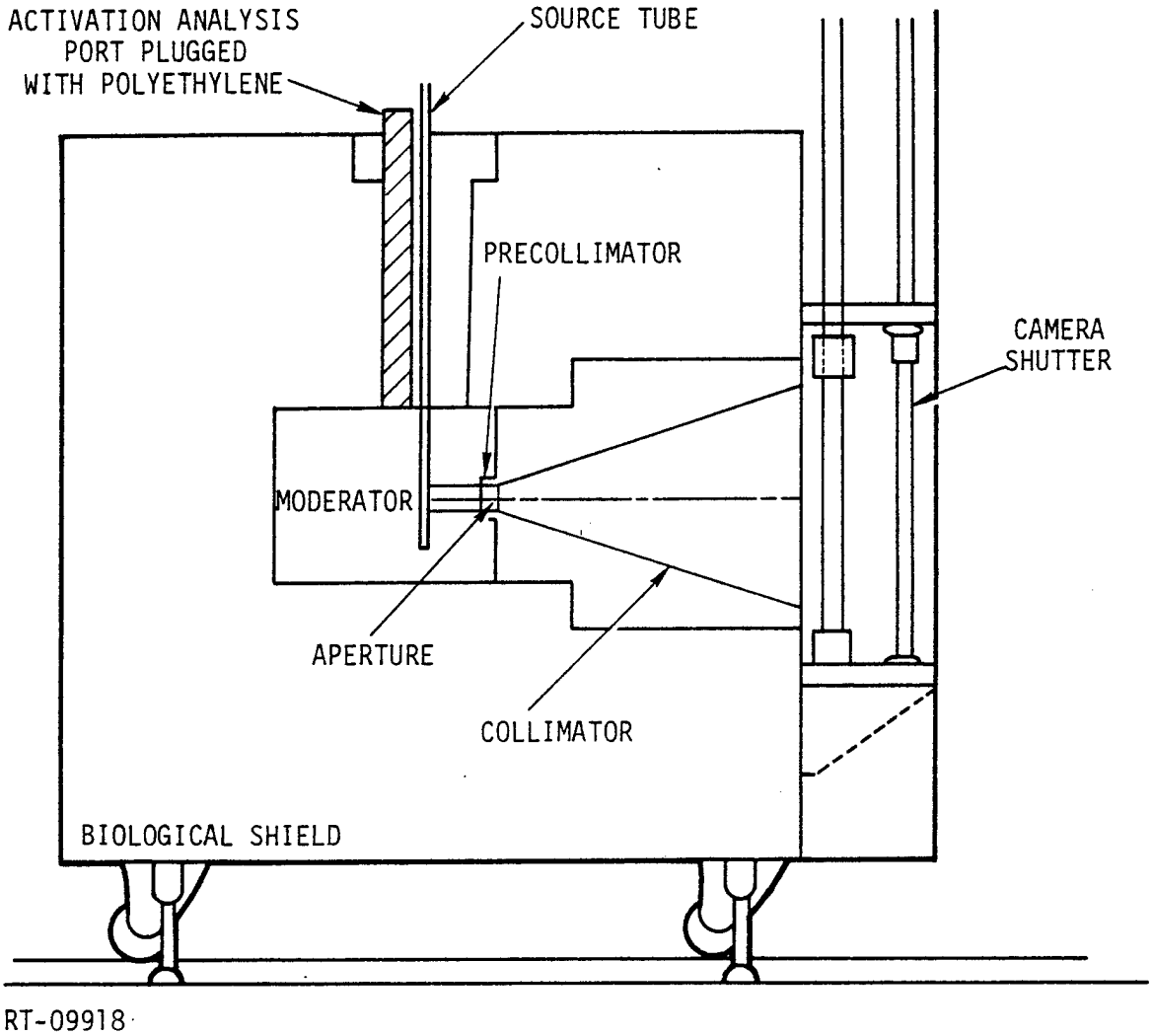

Figure 2. Neutroscope

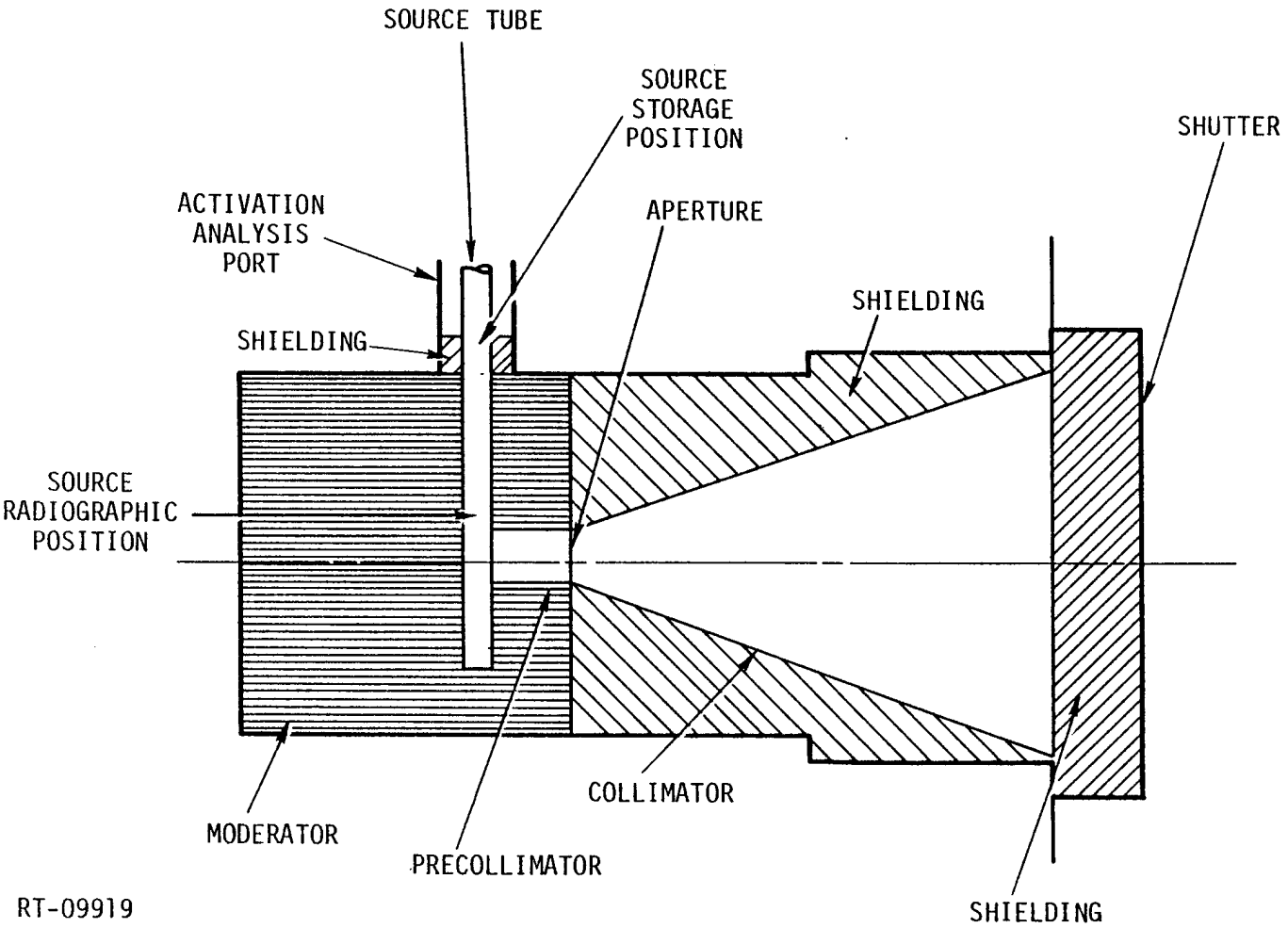

Figure 3. Moderator, precollimator, collimator, shutter

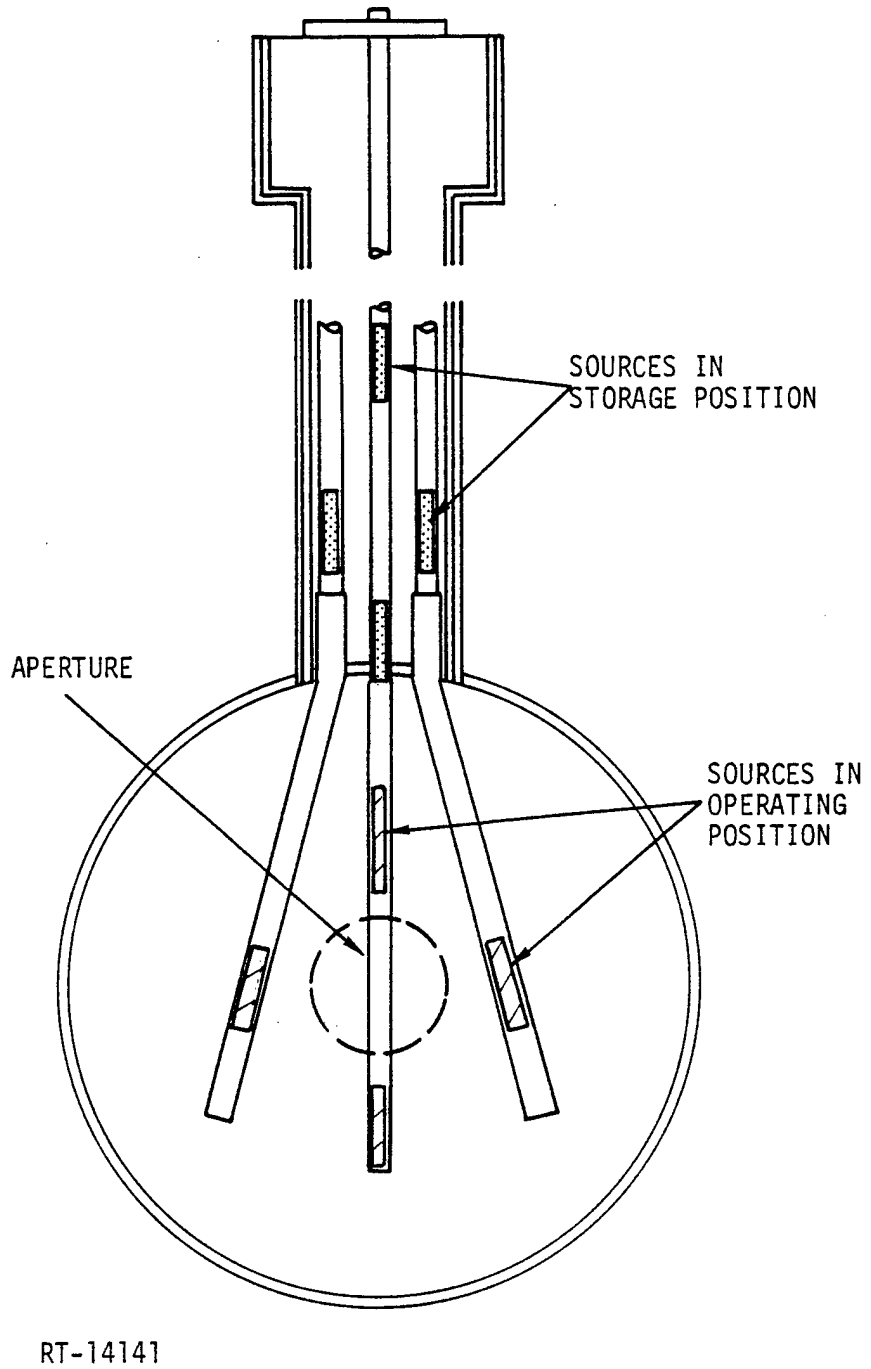

Figure 4. CFNR-10 source and moderator section showing arrangement for four ^{252}Cf sources in operating (hatched area) and storage position

3.1.2 Imaging System

This system consists of a cassette holder and a flexible cassette with a converter system. The flexible cassette holder consists of two pieces of thin aluminum sheet, within which is the converter, a 0.001-inch sheet of gadolinium, and the appropriate film. The edges of the cassette are light sealed with an opaque tape.

It was imperative that a flexible cassette be used for this study, since maximum resolution is achieved when the defect to film imaging system distance is minimal. Since the blades have a large overall curvature, this necessitates using a cassette with an appropriate flexibility. Also, the cassette had to physically fit in the area between the root section and blade shroud to be in intimate contact with the blade surface.

3.1.3 Beam Stop

The beam stop is a movable wall constructed of shielding materials to reduce the radiation dose from the neutron beam reaching the walls directly in the beam path. This unit has been designed to reduce the radiation from the neutroscope, with the shutter open, to less than 50 mrem/hr on the exiting surface of the beam stop.

3.2 OPTICAL MICROSCOPE

An American Optical microscope containing a calibrated grid was used to obtain the dimensions of the crack width. It had a maximum sensitivity of 0.0008 inch per division.

3.3 ENHANCEMENT TECHNIQUES

This section describes the two methods used to enhance the detection of defects in the compressor blades for neutron radiography.

3.3.1 Penetrant Enhancement Techniques

As mentioned previously, in this technique the goal is to fill the crack with a material having a large thermal-neutron absorption coefficient.

The method used to achieve this is schematically shown in Figure 5. The areas of interest on the compressor blades are immersed in an enhancing agent. This enhancing agent is designed to have low surface tension. The container with the penetrant is also in a larger vessel capable of being evacuated and pressurized.

Initially, the larger vessel is evacuated to remove the air present in the cracks. The unit is then pressurized up to several atmospheres to force the penetrant solution into the cracks. This process is repeated several times. Upon removal from the penetrant solution, the blades must be carefully wiped of the residual penetrant solution. This is necessary to prevent the deposition of the solute on the surfaces when the solvent evaporates. Since the penetrant's sole function is to be detected, any undesirable residue would easily be detected.

3.3.2 Electrodeposition Enhancement Technique

In this technique, the objective is to electroplate a material with a large thermal-neutron absorption coefficient on those areas surrounding the cracks. After some preliminary investigations, gadolinium was successfully electroplated on titanium. A microprobe analysis substantiated that the deposited layer was predominantly gadolinium.

Prior to electroplating, the immediate areas around the crack were chemically etched clean. A dilute solution of hydrofluoric and nitric acid applied locally with a cotton swab was very effective for this, followed immediately by rinsing with copious quantities of water. A final rinse with acetone left the surface in a clean condition, ready for electroplating. By only locally cleaning the areas of interest, it was not necessary to mask any other areas of the blade, since no deposit would adhere to an unclean surface.

A plating current of approximately 200 mA proved to be a satisfactory value. Excessive platting currents gave depositions resulting in coarse, granular structures not desirable for radiography purposes. Best results were obtained when the blade (cathode) remained stationary, and the stainless probe (anode) was successively passed slowly over the area to be plated.

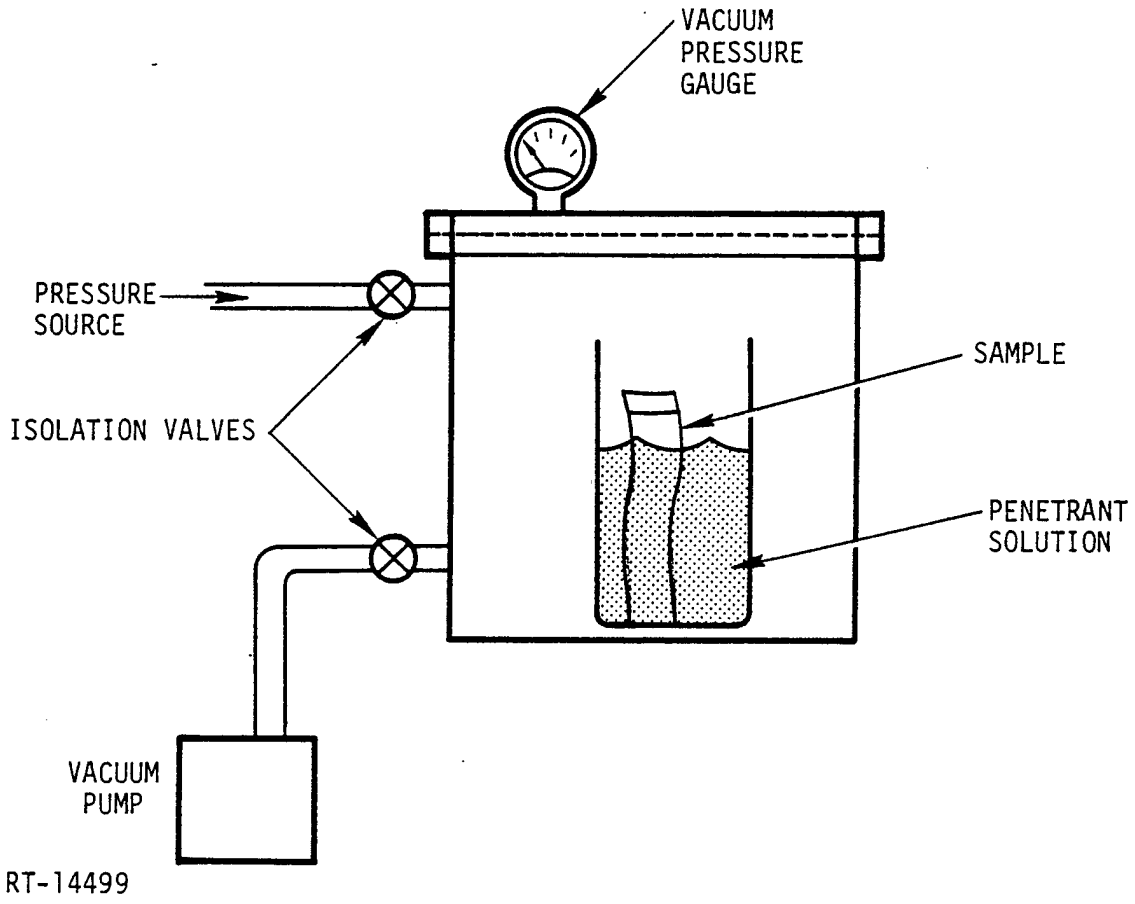

Figure 5. Schematic of system used for penetrant technique

By doing the electroplating in a glass beaker, one could observe the progress of the deposition and determine when to terminate the process. Generally, the plating times were on the order of several minutes for a satisfactory deposition. For this study, both sides of the blade were electroplated.

After removal from the plating solution, the blade must be thoroughly washed and rinsed of the plating solution, since the solution is the same as used for the penetrant technique. It is obviously imperative that the crack be free from the penetrant, or the net desired effect may be nullified.

3.4 SPECIMENS

A series of 12 titanium engine blades were examined in this study. Figure 6 shows a schematic of a typical turbine blade with an observable defect.

It was imperative to concentrate on cracks that were visually observable so that the crack width and length could be quantitized. The reference distance, x_1, is the distance to the crack from the leading edge corner of the root portion of the blade, and is used to locate the defect along the longitudinal axis.

3.5 CHEMICAL EFFECTS OF ENHANCING AGENTS ON THE BLADE

Extensive tests had previously been conducted to examine the chemical effects of the penetrant solution on titanium-based materials. During these tests, the components were maintained at elevated temperatures for extended periods of time. There was no evidence of any deleterious effects on the titanium resulting from the application of the penetrant solution.

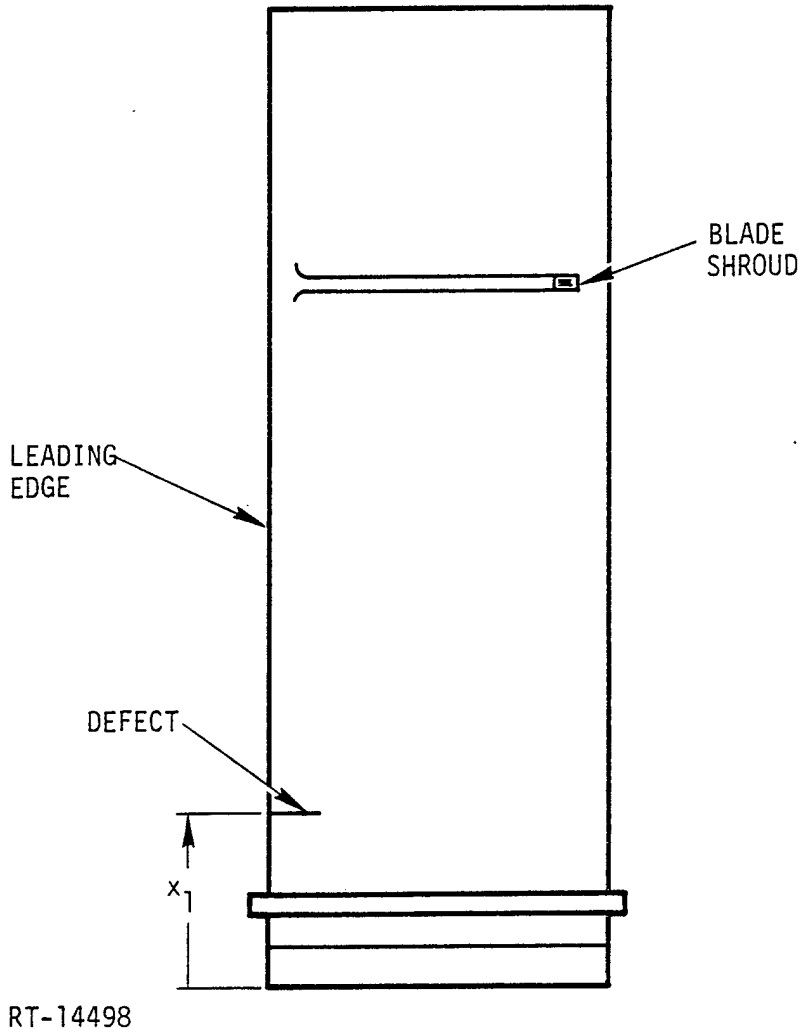

Figure 6. Schematic of compressor blade showing reference distance (x_1) to locate defect

4. EXPERIMENTAL PROCEDURES

The experimental procedures used to obtain neutron radiographs of the compressor blades will now be outlined.

a. Clean compressor blades

All blades were ultrasonically cleaned first in a detergent solution, and then in acetone.

b. Visually inspect blades

Each blade was carefully examined microscopically and the particulars of the observed defects were recorded. This included the location of the defects with respect to the leading edge, an approximation of the crack width and length, and any other significant details of interest.

c. Photograph entire blade and take a closeup of observed areas of suspicion

Black-and-white photographs were taken for record purposes, which included close-up photos of those defects visually observable.

d. Neutron radiograph the blades in their "as-received" condition

These radiographs would represent the reference radiographs when comparing to those with the penetrant and electroplated materials.

e. Impregnate blades with the gadolinium penetrant solution

Using the methods described previously, vacuum and pressure impregnate the defects with the gadolinium salt solution.

f. Neutron radiograph the blades with penetrant solution.

g. Wash blades free of penetrant solution

In order to return to the "as-received" condition, the penetrant must be removed from the defects. This is readily achieved by thoroughly washing the blades in hot running water, followed by a final rinse with acetone.

h. Neutron radiograph the blades to verify removal of penetrant material.

i. Chemically etch the areas of interest in preparation for electroplating

It was experimentally determined that this etching process should be done just prior to electroplating for best results.

j. Electroplate gadolinium on the areas of interest.

k. Completely wash blades to remove residual penetrant, particularly from the defects.

l. Neutron radiograph electroplated areas.

m. Chemically remove the plated gadolinium, and do a final cleaning prior to completing the neutron radiography phase of work.

5. EXPERIMENTAL RESULTS AND ANALYSIS

The experimental results are shown in Figures 7 through 18 inclusive. These are black-and-white positives of the original radiographs. Shown in each figure are the blade sections in the as-received state with no penetrant or deposition (H852), that with the penetrant applied (H849), and that with the electrodeposited material (H853). Evident in the positive copies of the neutron radiographs are striations caused by the gadolinium foil to film distance being a variable. This condition is often present in flexible cassettes of the type used for this experiment, due to the difficulty of completely eliminating the distance between converter and film.

Table 2 lists all of the pertinent data from the radiographs examined. The numbers listed in the column titled "Defect I.D." were arbitrarily assigned to the defects studied, and used solely for identification.

Except for compressor blades "H" and "29", all defects extended in from the edges of the blades, normal to the longitudinal axis of the blade. For blade "H", no observable cracks were visually discernable. The other exception, blade "29", had cracks that appeared to be superficial in nature and were located near the center of the top portion of the blade. Their orientation was similar to those in the other blades, but the cracks did not visually extend to the edge. The results of defect detectability, i.e., being able to see a response on the film, were based on examining the original radiograph and not the copies, since some detail is invariably lost when producing copies. For the results of defect detectability, a "yes", "no", or "uncertain" corresponds to being definitely able to see a response, not seeing a response, and being uncertain of a response, respectively. The latter condition exists in some instances, since we know where the defect should be, but artifacts are present on the film that may or may not be a response due to the defect.

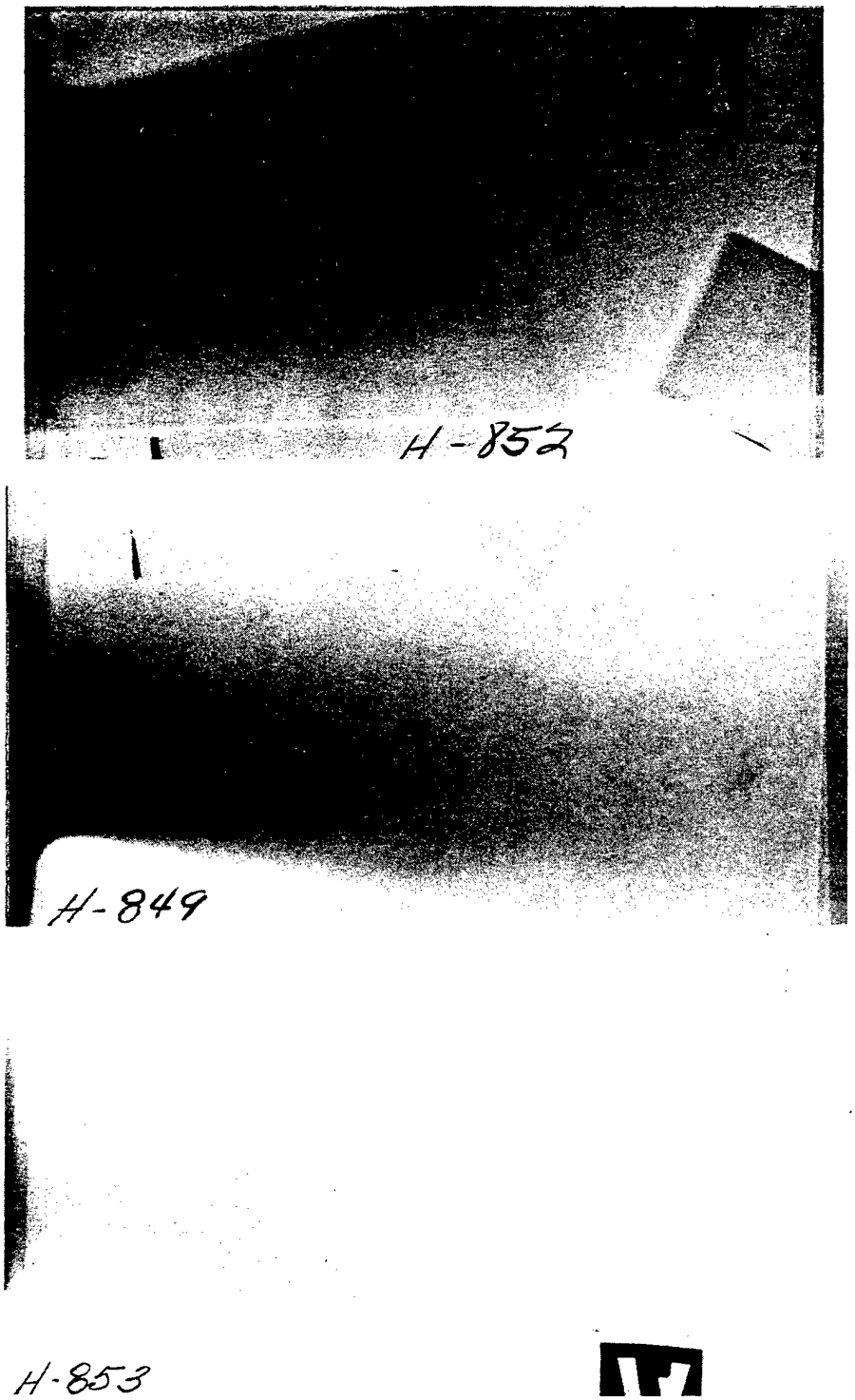

Figure 7. Copies of neutron radiographs for compressor blade A in its as-received condition (H852), with penetrant (H849), and with electro-deposited material (H853)

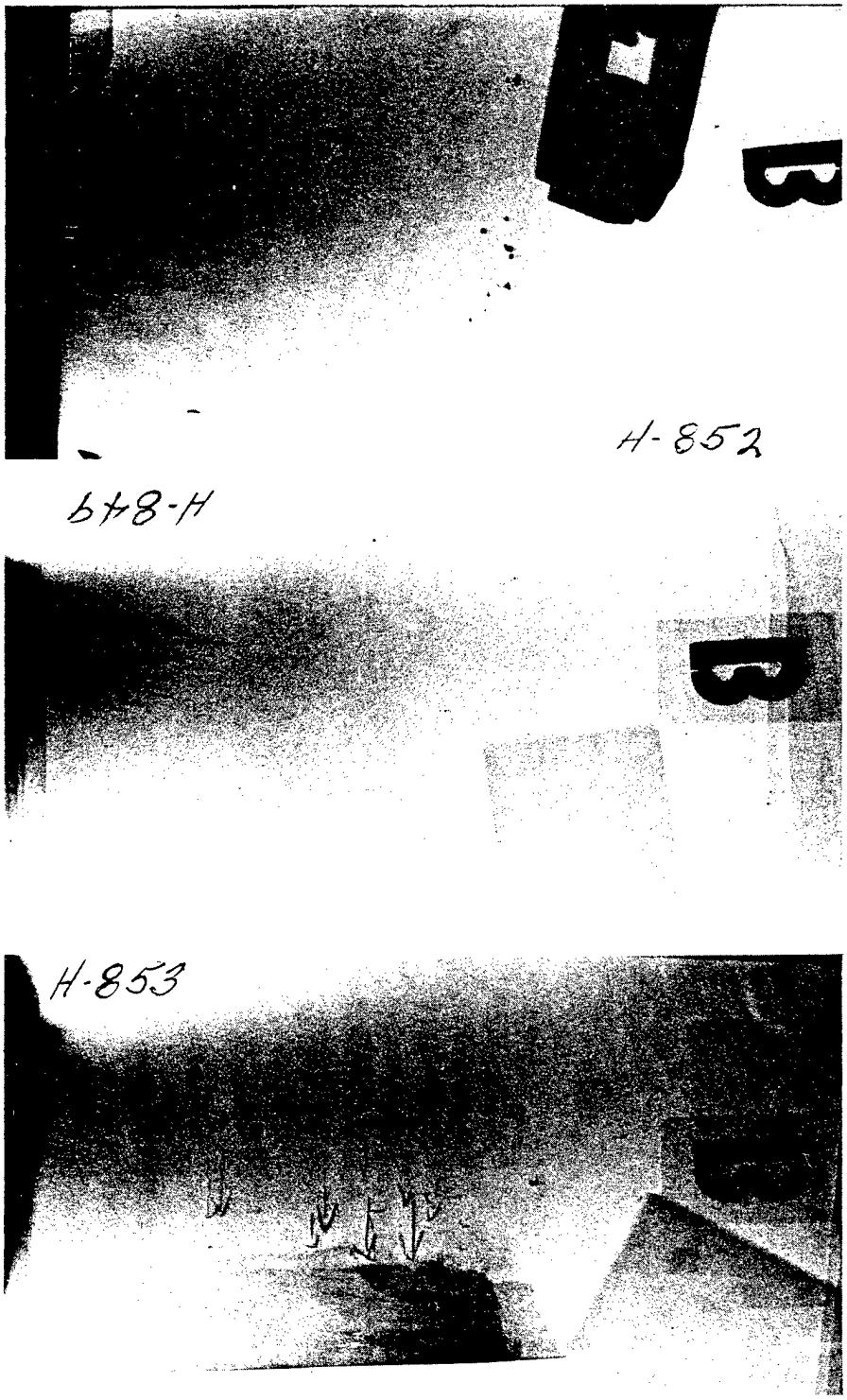

Figure 8. Copies of neutron radiographs for compressor blade B in its as-received condition (H852), with penetrant (H849), and with electro-deposited material (H853)

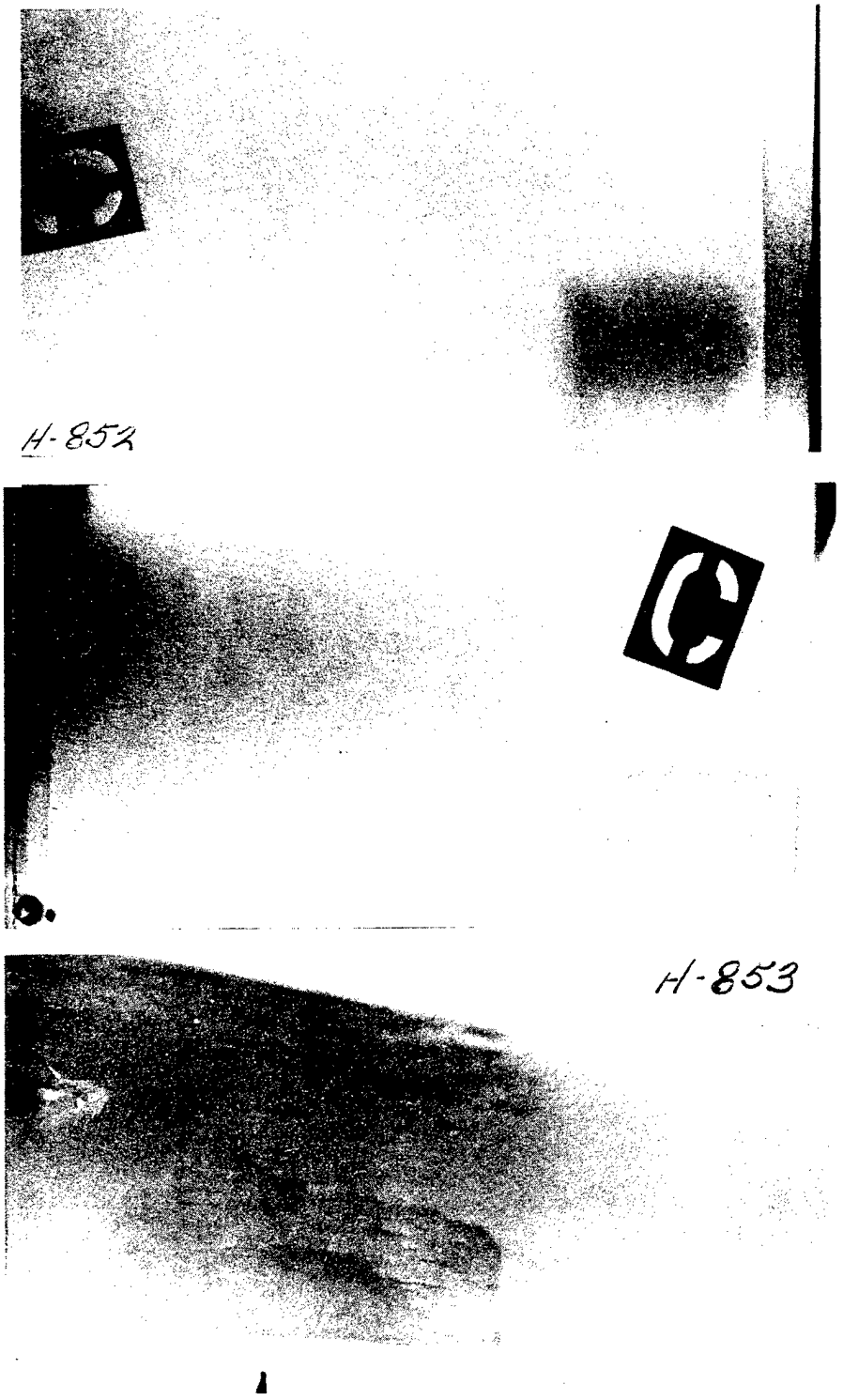

Figure 9. Copies of neutron radiographs for compressor blade C in its as-received condition (H852), with penetrant (H849), and with electro-deposited material (H853)

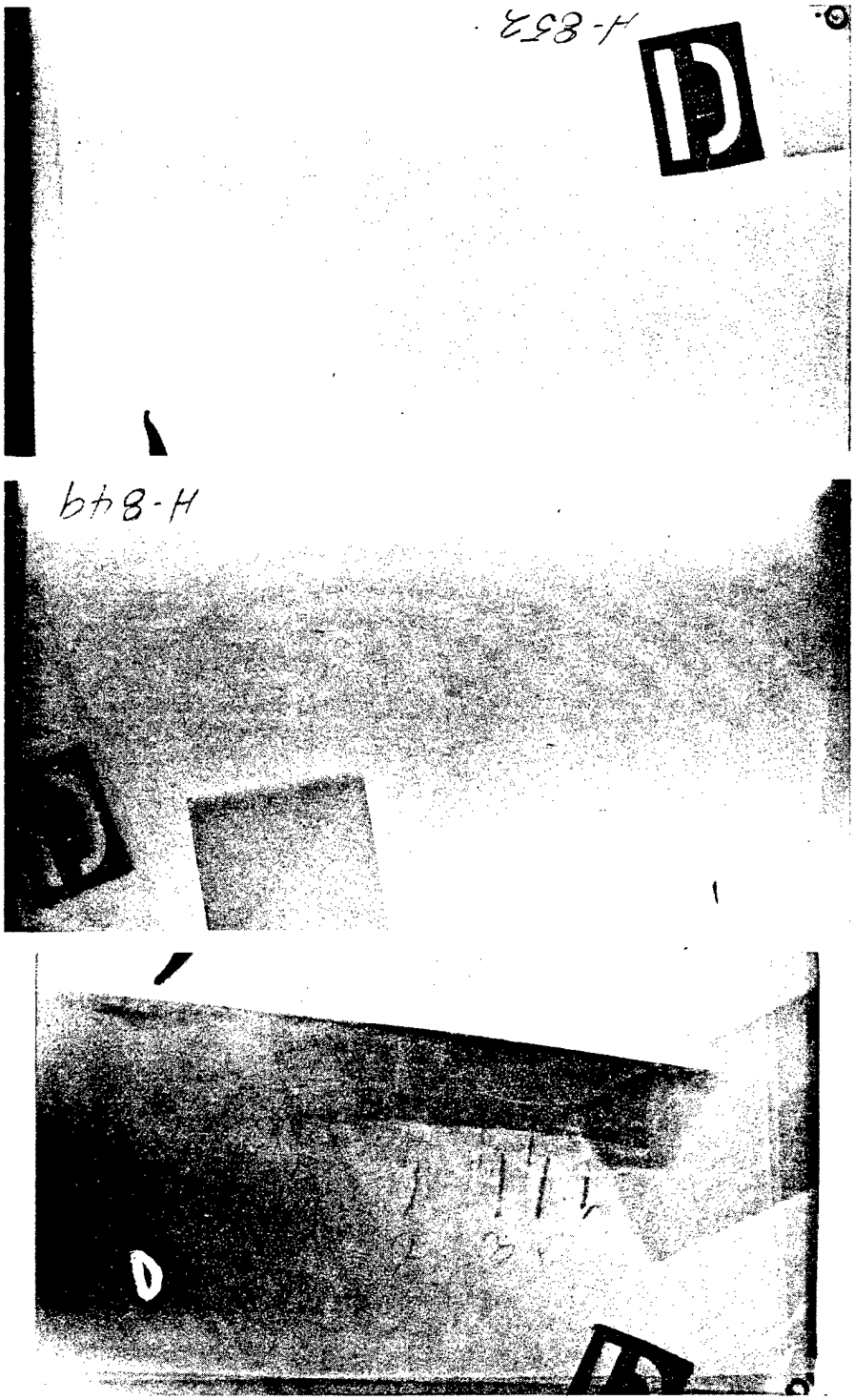

Figure 10. Copies of neutron radiographs for compressor blade D in its as-received condition (H852), with penetrant (H849), and with electro-deposited material (H853)

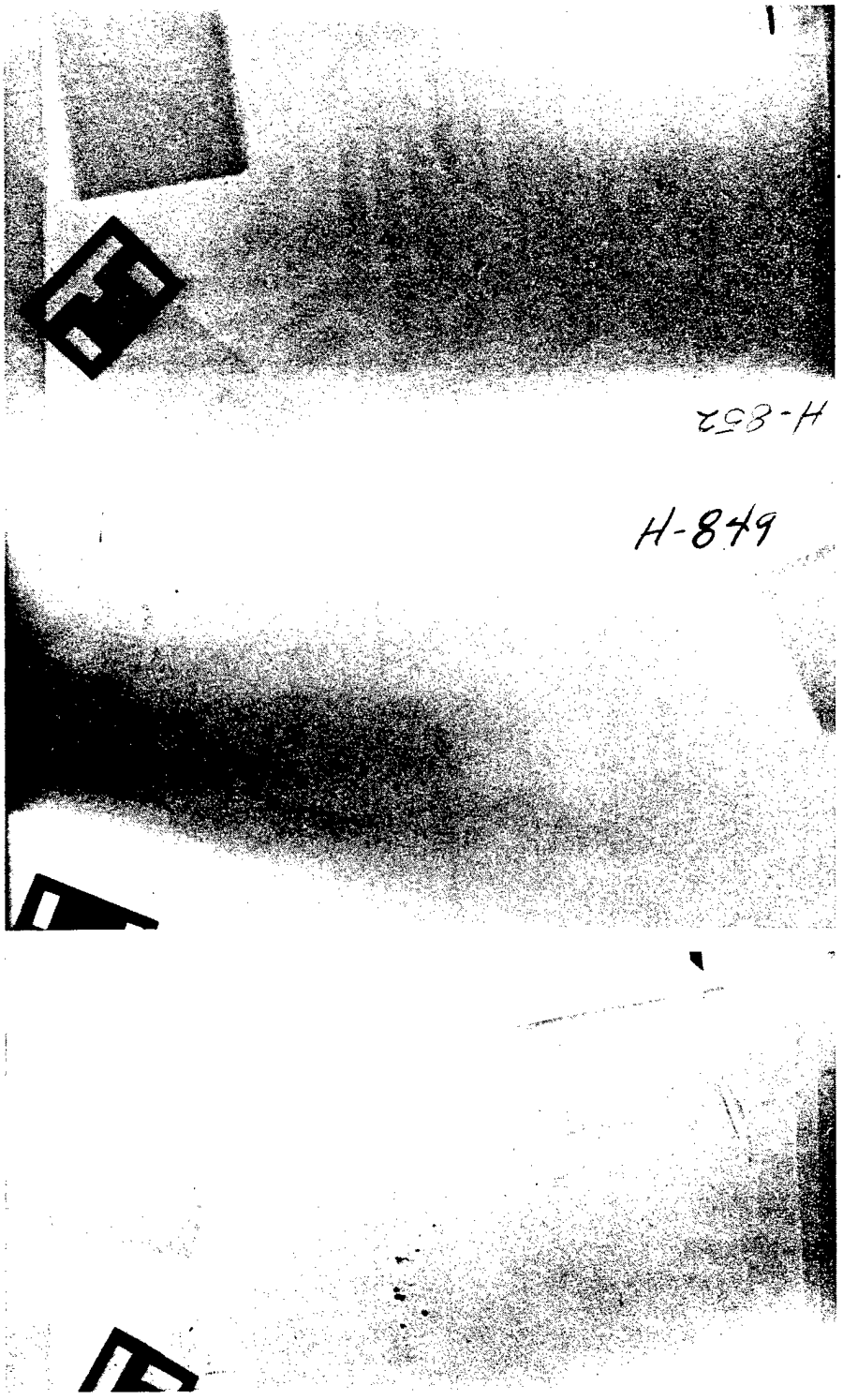

Figure 11. Copies of neutron radiographs for compressor blade E in its as-received condition (H852), with penetrant (H849), and with electro-deposited material (H853)

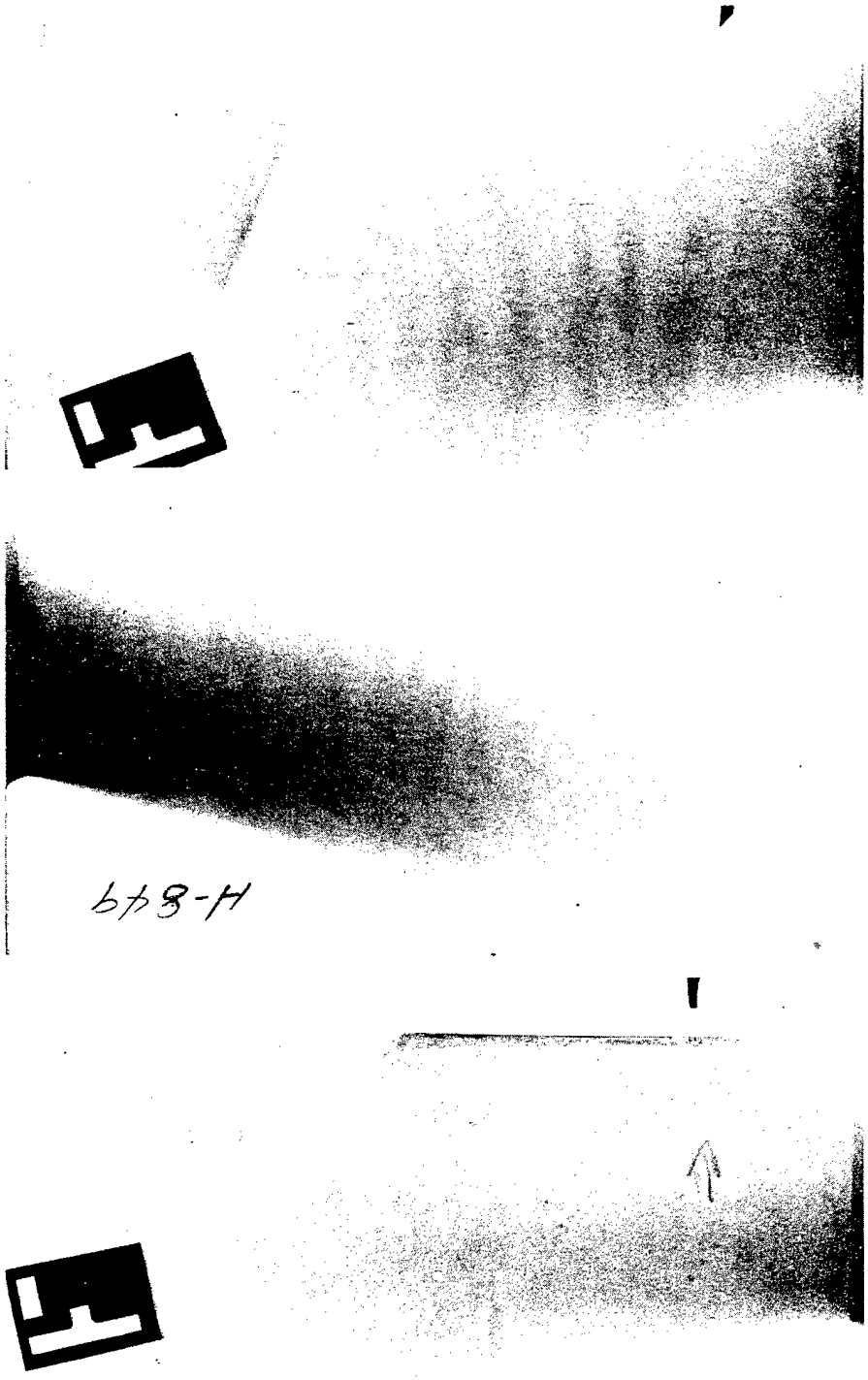

Figure 12. Copies of neutron radiographs for compressor blade F in its as-received condition (H852), with penetrant (H849), and with electro-deposited material (H853)

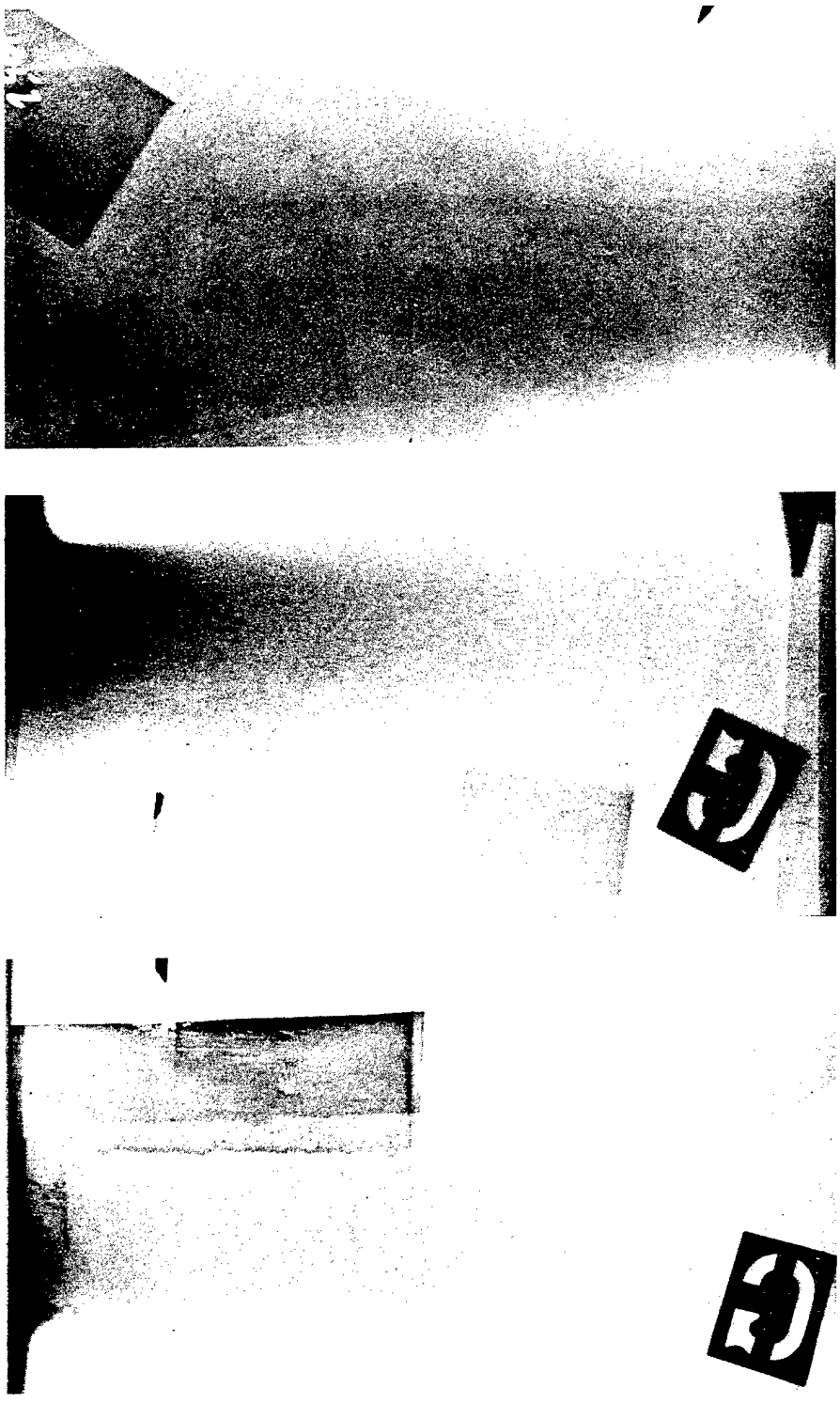

Figure 13. Copies of neutron radiographs for compressor blade G in its as-received condition (H852), with penetrant (H849), and with electro-deposited material (H853)

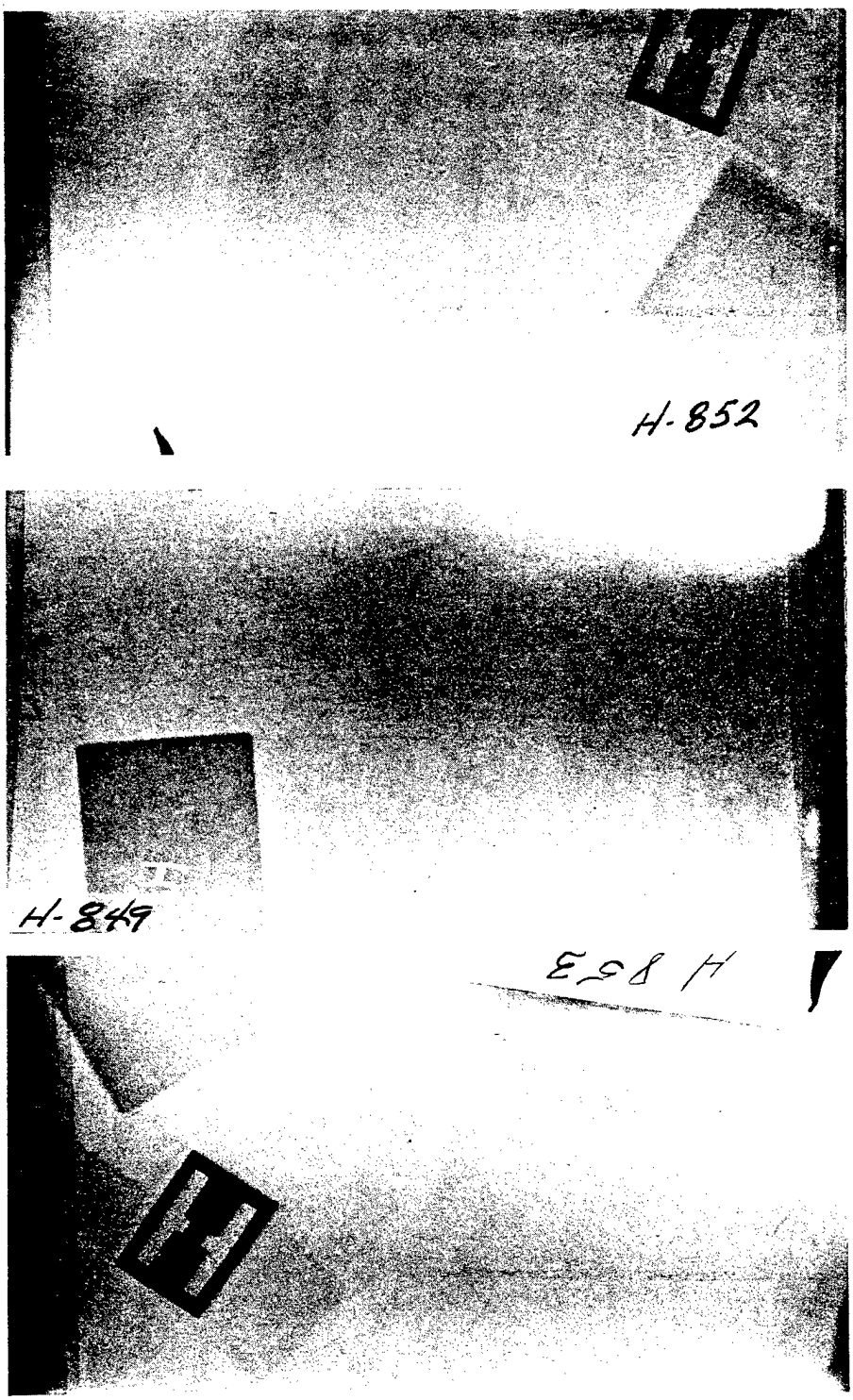

Figure 14. Copies of neutron radiographs for compressor blade H in its as-received condition (H852), with penetrant (H849), and with electro-deposited material (H853)

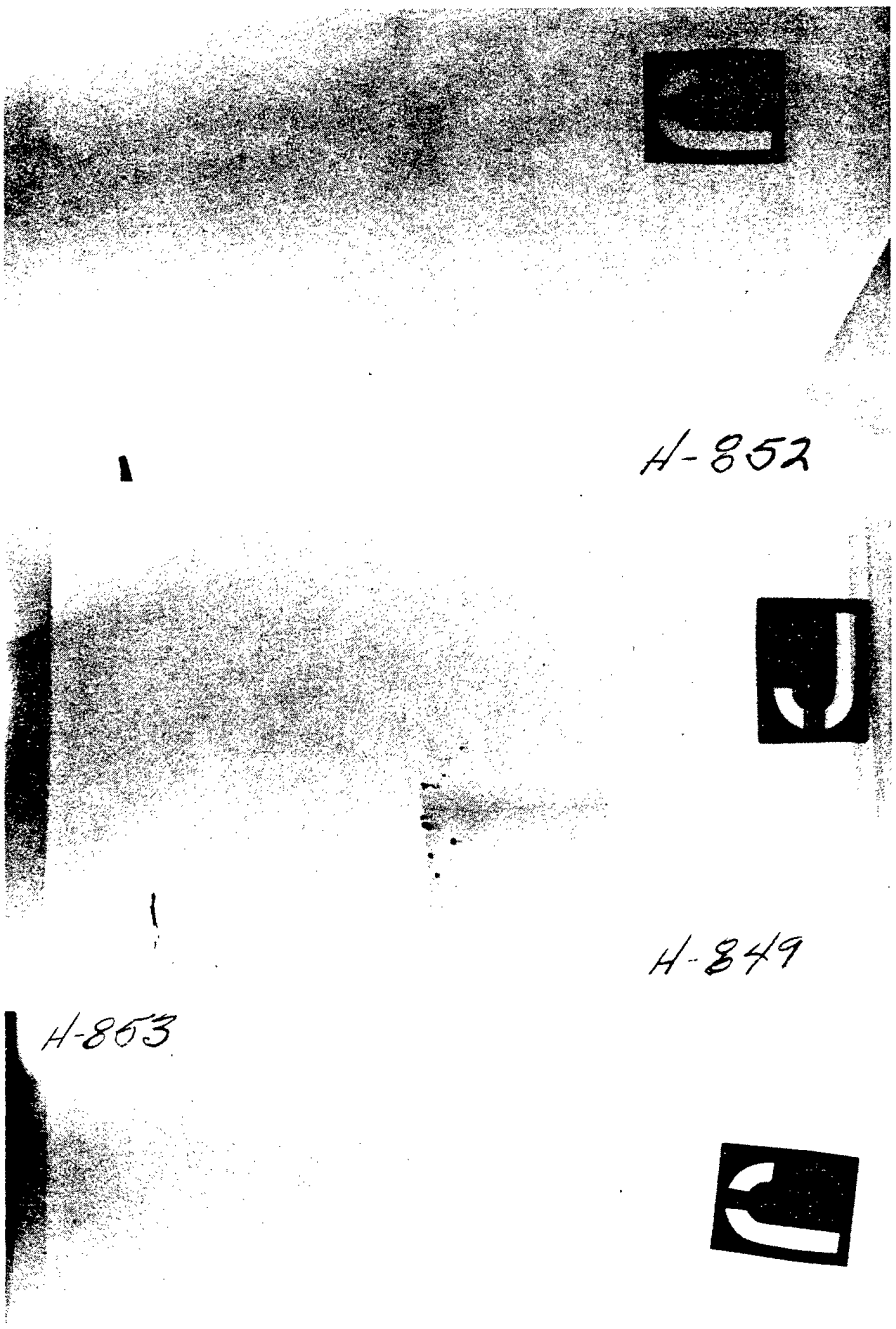

Figure 15. Copies of neutron radiographs for compressor blade J in its as-received condition (H852), with penetrant (H849), and with electro-deposited material (H853)

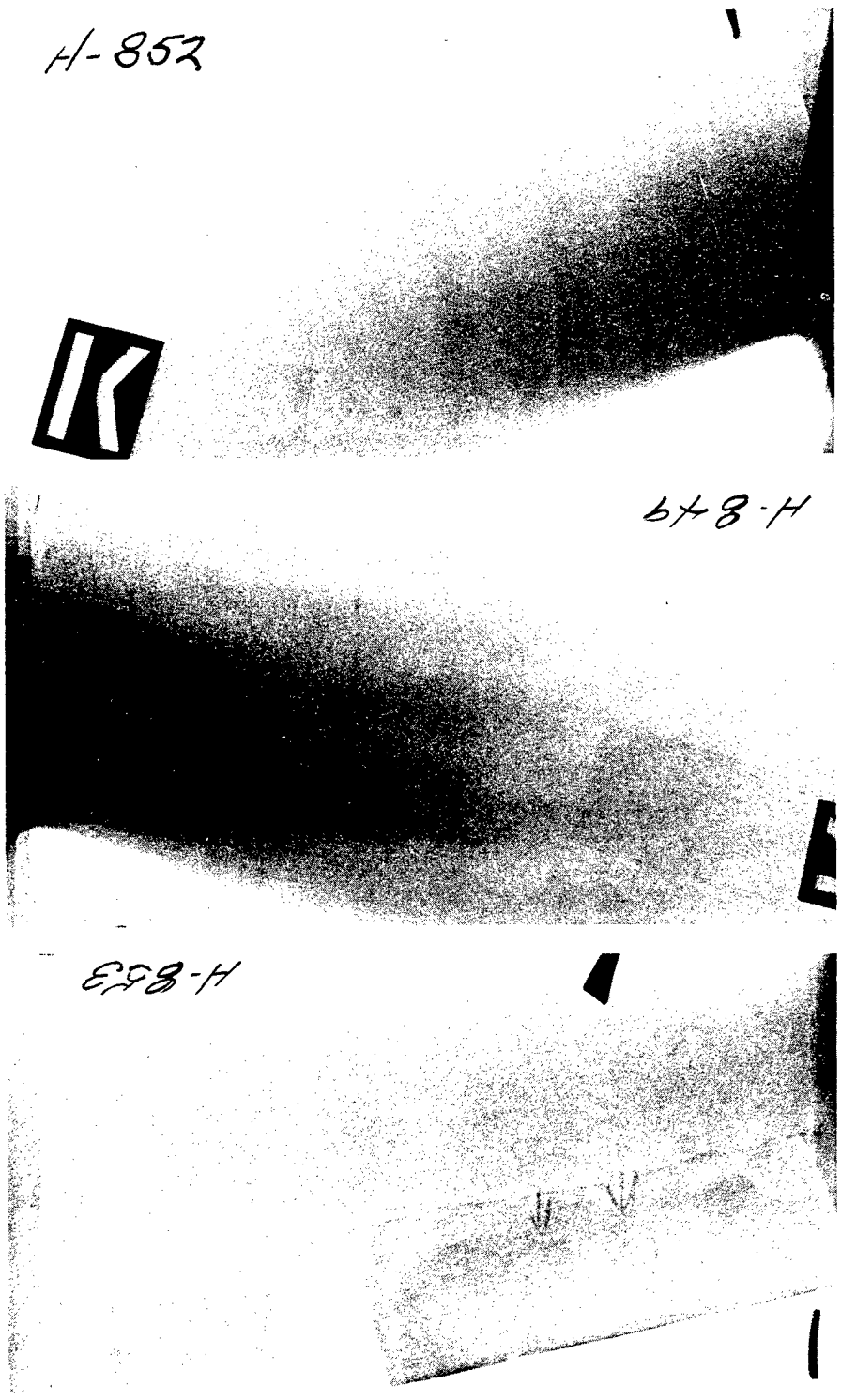

Figure 16. Copies of neutron radiographs for compressor blade K in its as-received condition (H852), with penetrant (H849), and with electro-deposited material (H853)

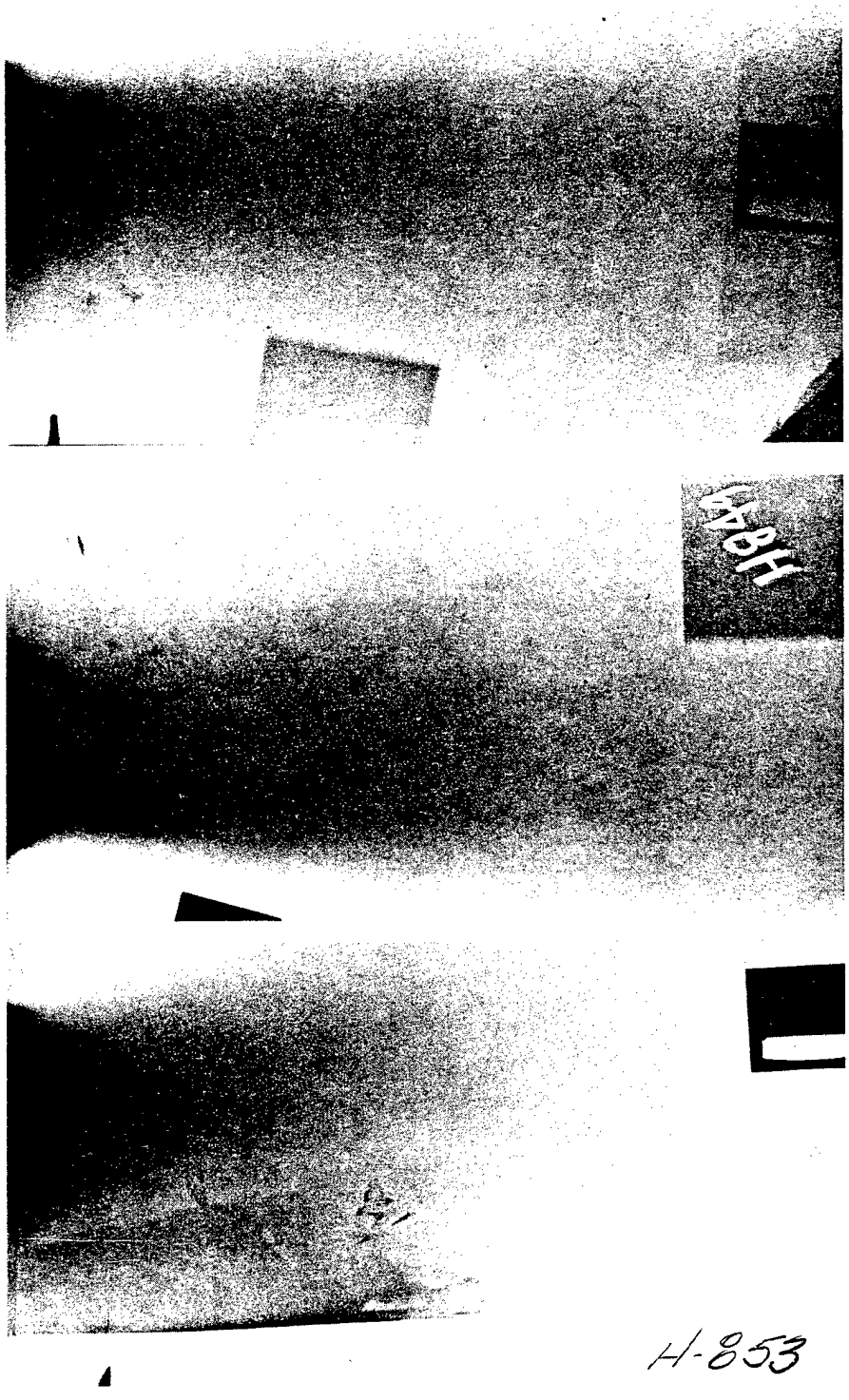

Figure 17. Copies of neutron radiographs for compressor blade L in its as-received condition (H852), with penetrant (H849), and with electro-deposited material (H853)

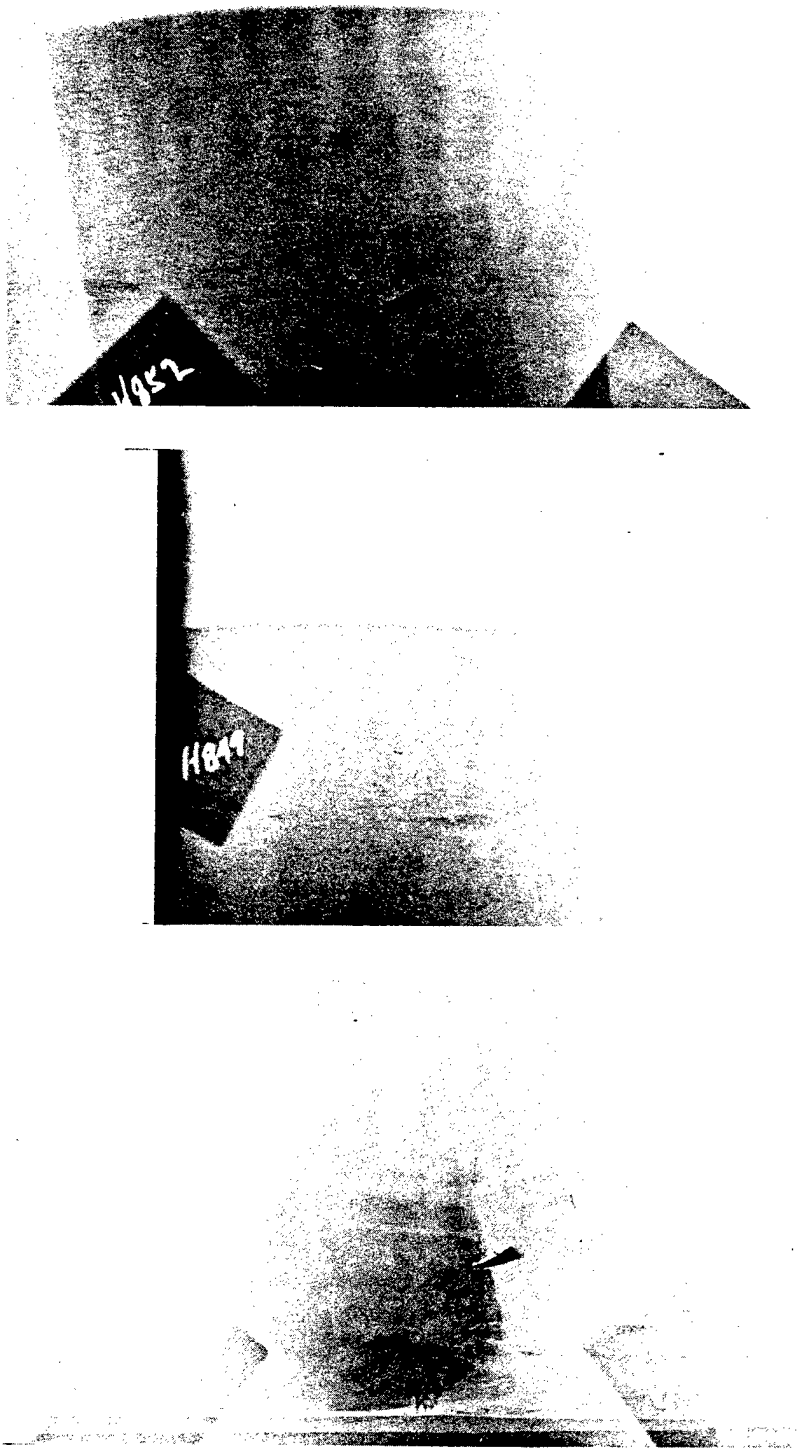

Figure 18. Copies of neutron radiographs for compressor blade 29 in its as-received condition (H852), with penetrant (H849), and with electro-deposited material (H853)

Table 2

SUMMARY OF DEFECT DETECTABILITY IN TITANIUM COMPRESSOR BLADES UTILIZING NEUTRON RADIOGRAPHY

Blade I.D. No.	Defect Parameters				Defect Detectability		
	Defect I.D.	Ref. Distance (inches)	Crack Length (mils)	Crack Width (mils)[a]	Non-Enhanced	Penetrant	Electroplated
A	1	1.7	200	4	Yes	Yes	Yes
B	1	0.95	200	<0.3	No	No	No
	2	2.1	20	<0.3	No	No	?
	3	2.65	20	<0.3	No	No	?
	4	3.08	20	<0.3	No	No	?
	5	3.20	20	<0.3	No	No	?
C	1	2.8	100	<0.3	No	No	No
D	1	1.9	100	2	Yes	Yes	Yes
	2	3.6	∿20	<0.3	No	No	?
	3	4.1	∿20	<0.3	No	No	?
	4	4.3	∿20	<0.3	No	No	?
	5	4.5	∿20	<0.3	No	No	?
E	1	1.5	200	1.5	Yes	Yes	Yes
F	1	1.95	50	∿0.5	Yes	Yes	Yes
G	1	1.95	200	4	Yes	Yes	Yes
H	1	1.3	---	---	No	No	No
J	1	1.8	300	4	Yes	Yes	Yes
K	1	1.05	150	0.3	No	Yes	No
	2	2.10	25	0.3	No	Yes	No
	3	2.40	25	0.3	No	Yes	No
	4	2.80	25	0.3	No	Yes	No
L	1	1.6	100	1	?	Yes	Yes
	2	1.85	10	0.3	No	Yes	Yes
	3	2.10	14	<0.3	No	No	No
#29	1	10.4	300	∿0.5	No	No	No
	2	10.5	200	∿0.5	No	No	No

[a]Indicated crack widths stated as <0.3 mil may actually be <<0.3 mil since actual measurements in this area are complicated by the erratic nature of crack interfaces.

6. SUMMARY OF RESULTS

The results are summarized and presented in Table 2, and some of the salient features that were observed are now summarized.

6.1 DEFECT DETECTABILITY FOR EACH CONDITION

a. Without the use of any enhancement technique, some cracks in titanium blades can be observed on a neutron radiograph. The smallest crack that was observed (E-1), had a width ∿1.5 mils wide and 200 mils long. Cracks smaller than this (L-1), were considered to be uncertain, and those with widths larger but of shorter length (D-1), could be detected.

b. Utilizing a gadolinium salt penetrant, smaller cracks could be observed. Cracks with a width ∿0.3 mil wide and 10 mils long (L-2), could be observed.

c. Utilizing an electroplated layer of gadolinium over the defect area similarly enhanced the detection of the crack as compared to the nonenhanced condition. A crack with a width of ∿0.3 mil and 10 mils long (L-2), was detected.

6.2 DEFECT DETECTABILITY COMPARISON BETWEEN THE ENHANCEMENT TECHNIQUES

When comparing the two different enhancement techniques, the following can be observed.

a. Excluding the "uncertain" results, the penetrant enhancement technique appears to be more effective. This is particularly evident for blade K.

b. If one considered the "uncertain" results, there are indications that the electroplating technique may have some merit. This is seen for blades B and D.

7. CONCLUSIONS

The main conclusions resulting from this study can be summarized as follows.

a. Neutron radiography utilizing thermal neutrons can successfully be used to detect cracks in titanium-based compressor blades.

b. Without the use of any enhancement techniques, cracks with widths on the order of 1.5 mils and 200 mils long can be detected.

c. With the use of either enhancement technique, cracks having widths on the order of 0.3 mil and 10 mils long can be detected.

8. RECOMMENDATIONS

Based on the results reported here, the following recommendations are made.

a. Conduct a parametric study to clearly define the detectability of cracks using this technique. Using a statistically significant number of samples, carry out an experimental analysis to determine the probability of detecting cracks as a function of crack dimensions.

b. Examine the probability of accelerating the admittance of the enhancing agent by "working" the blades while applying the enhancing agent.

c. Evaluate additional enhancing agents with lower surface tension and viscosity to penetrate smaller cracks.